Anal. Bioanal. Electrochem., Vol. 15, No. 5, 2023, 394-409
https://www.doi.org/10.22034/abec.2023.705137

Analytical &
Bioanalytical
Electrochemistry

2023 by CEE
www.abechem.com

Full Paper

Peganum Harmala Seeds as A Sustainable Source of Pickling Inhibitor for Zinc: Anti-Oxidant Properties, Adsorption Behaviour, Electrochemical Studies, and Synergistic Effect

Mina Boulkroune,[1,2,*] Bilel Dekkiche,[2] and Yaaqoub Abassi[2]

[1]*Environmental and Structural Molecular Chemistry Research Unit (UR-CHEMS), Faculty of Exact Sciences, University Constantine 1, Constantine 25000, Algeria*
[2]*Department of Chemistry, Faculty of Exact Sciences, University of Constantine 1, Constantine 25000, Algeria*

*Corresponding Author, Tel.: +2135151965575
E-Mail: minaboulkroune@yahoo.fr

Received: 14 January 2023 / Received in revised form: 16 May 2023 /
Accepted: 20 May 2023 / Published online: 31 May 2023

Abstract- The presence of various antioxidants in the ethanolic extract of Peganum harmala L. (EEH) seeds with different oxidation potentials was confirmed by cyclic voltammetry. The evaluation of the inhibition efficiency of the extract on zinc corrosion in the hydrochloric acid medium was carried out by gravimetry and electrochemical techniques. The results showed that the extract has satisfactory corrosion-inhibiting properties and that its efficiency is controlled by its concentration and medium temperature. The inhibition rate reached 96.8% in the presence of 2200 ppm of the EEH extract at 298K. The potentiodynamic polarization study showed that the extract is classified as a mixed-type inhibitor with a cathodic predominance. A good agreement between the results of the gravimetric study and those of the electrochemical measurements was demonstrated. The studied extract acts by physical adsorption, as indicated by the thermodynamic parameters, and follows the Langmuir model. The inhibition efficiency of the studied extract was improved in the presence of KI through a synergistic effect.

Keywords- Pickling inhibitors; Green inhibitors; Peganum harmala; Anti-oxidants; Zinc

1. INTRODUCTION

Acid corrosion inhibitors are used in different industrial processes like cleaning and pickling metals. The majority of the inhibitors used are synthetic products, which offer good protection against the corrosion of metallic materials. But most of them are toxic and can affect the environment. The search for new corrosion inhibitors has currently undergone considerable development, and research is oriented toward green inhibitors. The use of plant extracts as corrosion inhibitors is a research topic in development. Indeed, plants contain a complex mixture of natural organic compounds and constitute an ecological, available, and renewable source for green inhibitors. The tests carried out on the anticorrosive properties of natural products extracted from *Lawsonia* leaves [1], *Azadirachta indica* [2], *Cuminum ciminum*, and *Pimpinella anisum* seeds [3] have shown promising results for zinc in hydrochloric acid, knowing that this metal is very sensitive to acids and corrodes easily in acidic environments [3]. It has been found that the corrosion inhibition capacity of plant extracts is attributed to the antioxidant properties of phytochemicals [4,5]. The importance of this field of research is mainly related to the fact that natural products can substitute toxic organic molecules.

Peganum harmala is a plant of the Zygophyllaceae family. It is largely distributed throughout the world, and widely used in traditional medicine.

Among the constituents of this plant, we find flavonoids, amino acids (valine, phenylalanine, glutamic acid, threonine, proline, and histidine), sterols/triterpenes, volatile bases, coumarins, and tannins [6]. It also contains alkaloids such as Harmine, Harmaline, Harmalol, and Harmane [7].

Studies carried out on the use of *Peganum harmala* seeds extracts for corrosion protection of 6063 aluminium alloy [8] and mild steel [9] in HCl solutions, and carbon steel in HCl [10], H_2SO_4 [11], and NaCl [12] solutions, and also the Harmal leaves, roots, and flowers extracts for carbon steel protection in H_2SO_4 solutions [13,14], showed satisfactory results. A review of the literature showed that no research has been devoted to the use of *Peganum harmala* seeds as a source of pickling inhibitor for zinc.

A theoretical study reported that the main alkaloids present in Harmal seeds have anticorrosive properties, and their inhibition efficiencies rank in the following order: Tetrahydroharmine < Harmine < Harmalacidine < Harmalol < Harmaline [10].

The aim of this work consists of evaluating the influence of Peganum Harmala seeds extract on zinc corrosion in a hydrochloric acid medium using weight loss and electrochemical methods.

2. EXPERIMENTAL SECTION

2.1. Materials

The study was conducted using pure zinc samples. For the gravimetric tests, square samples with an area of 2cm² were used. The electrochemical tests were performed using a working electrode prepared from a zinc sample, with an exposed surface of 0.405cm². For the reproducibility of the results, the samples were polished before each test with emery paper of different grades (400-600-1200-2000). The samples were washed with distilled water, degreased with acetone then rinsed with distilled water, and finally dried.

The corrosive medium was prepared from a commercial solution of HCl 36% hydrochloric acid, density d=1.18. Dilutions were made using distilled water.

Peganum harmala seeds were purchased from the market. 10g of the powdered plant material was mixed with 50 ml of ethanol. The mixture was left in the shade at room temperature for 48h, then filtered, and the filtrate was concentrated to dryness by evaporation of the solvent.

2.2. Gravimetric tests

The zinc samples used in the gravimetric measurements, and after being prepared according to the steps described above, are weighed, then fixed with plastic clips, and immersed in 25 ml of the solution for one hour.

At the end of the test, the samples are removed from the electrolyte, rinsed with distilled water and acetone respectively, and then air dried. Finally, the samples are weighed again. The weight loss tests were performed in 50 ml beakers placed in a thermostated bath allowing the electrolyte to be maintained at the desired temperature.

The surface coverage (θ) was calculated by the following formula:

$$\theta = [(CR_0 - CR_{inh}) / CR_0] \quad (1)$$

where CR_0 and CR_{inh} represent zinc corrosion rates in the uninhibited and inhibited solutions, respectively.

The corresponding inhibition efficiencies (IE) were determined using the equation:

$$IE(\%) = \theta \times 100 \quad (2)$$

2.3. Electrochemical tests

The electrochemical measurements were performed in a double-walled cell equipped with a conventional three-electrode system; SCE as a reference electrode, platinum as an auxiliary electrode, and a working electrode of glassy carbon (5mm diameter) for cyclic voltammetry tests and zinc for corrosion tests.

The capacity of the cell is 30ml, and a thermostated bath is used to control the temperature of the electrolyte.

The three electrodes are linked to a potentiostat / galvanostat / ZRA (GAMERY- reference 3000) controlled by the Gamery framwork software. The data processing was done with the Gamery Echem Analyst software.

Cyclic voltammograms were recorded at different scan rates from -0.2 to 0.9V/SCE in 0.1M phosphate buffer pH 7.0.

The polarization curves were plotted after a stable potential was reached. A potential scan in the range of -1.5 to -0.5V/SCE with a scan rate of 1mV/s was performed.

The inhibition efficiency values were calculated from the corrosion current densities of zinc in the uninhibited (I_{corr}) and inhibited ($I_{corr(inh)}$) solutions, using the following formula:

$$\mathrm{IE}(\%) = [(I_{corr} -_{(inh)})/I_{corr}]\times 100 \qquad (3)$$

Electrochemical impedance spectroscopy (EIS) experiments were carried out using AC signal at open circuit potential over a frequency range of 100 kHz-10 mHz and perturbation amplitude of 10 mV.

The inhibition efficiency values were calculated from the following equation:

$$\mathrm{IE}(\%) = [(R_{ct(inh)} - R_{ct})/ R_{ct(inh)}]\times 100 \qquad (4)$$

where R_{ct} and $R_{ct(inh)}$ are the charge transfer resistances without and with inhibitor, respectively.

3. RESULTS AND DISCUSSION

3.1. Electrochemical evaluation of antioxidant properties

Plants extracts are complex mixtures and can contain anti-oxidant substances that have great importance in different fields. Cyclic voltammetry is considered a simple and rapid electrochemical method that can be used to characterize the antioxidant properties of plant extracts [15,16]. The measured oxidation potential could be closely related to their antioxidant ability [17,18]. The cyclic voltammograms for 5000ppm of EEH extract shown in Figure 1 were recorded from -0.2 to 0.9 V/SCE at various scan rates (50, 100, and 200 mV.s^{-1}).

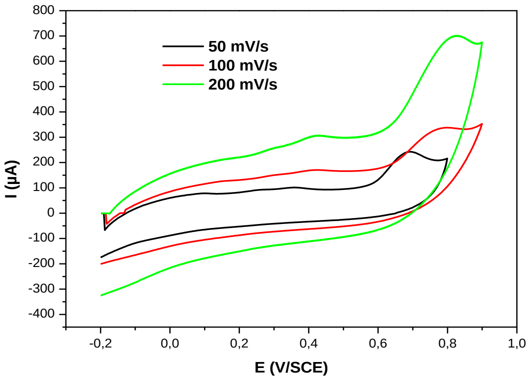

Figure 1. Cyclic Voltammograms of EEH extract in 0.1 M phosphate buffer pH 7.0 at various scan rates, using glassy carbon as working electrode

Two anodic peaks are observed, where the second one is more intense than the first. However, no cathodic peak is visible, indicating the irreversibility of the reaction [17]. The anodic peaks are related to the presence of various antioxidants, with different oxidation potentials. It means that the extract contains multiple antioxidants.

The anodic peaks currents (Ip_a) and the oxidation potentials (Ep_a) were determined and collected in Table 1.

Table 1. Electrochemical data determined from the voltammograms of 5000ppm EEH extract recorded at different scan rates

V ($mV.s^{-1}$)	Ep_{a1} (V/SCE)	Ip_{a1} (μA)	Ep_{a2} (V/SCE)	Ip_{a2} (μA)
50	0,360	101,3	0,693	242,6
100	0,424	170,5	0,800	337,7
200	0,428	307,3	0,828	701,6

Since low oxidation potential is related to the high antioxidant capacity [15], the high and low oxidation potential values determined from voltammograms reveal that the extract includes both compounds with an intermediate and good antioxidant capacity [19].

As the current is an additive magnitude, and since many unknown structures could occur in the extract, the amperometric current shows the contribution of several compounds included in the extract.

As shown in Table 1, the increase in the scan rate leads to a rise in the peak intensity as a result of the increase in sensitivity. We can also see a shift of the peak potential to higher values when the scan rate increases, showing that the oxidation process is irreversible [20].

3.2. Gravimetric measurements

3.2.1. Effect of concentration

In our study, we performed gravimetric measurements on zinc samples exposed to the corrosive solution at 298 K before and after the addition of various concentrations of Peganum harmala seeds extract (EEH). Table 2 shows the zinc corrosion rate, surface coverage values determined for different concentrations of EEH extract in 0.5 M HCl medium at 298 K, and the corresponding inhibition efficiencies.

The data in the table show that the studied extract inhibits the corrosion of zinc and reduces its dissolution rate.

The inhibition rate increases with the increase of the extract concentration in the corrosive medium and reaches 96.4% in the presence of 1800 ppm of the EEH extract. Above this concentration, the variation in efficiency is less significant.

Table 2. Zinc corrosion rates, surface coverages, and inhibition efficiencies for different concentrations of EEH extract in 0.5 M HCl medium at 298 K

	C (ppm)	**CR ($mg/\,h.cm^2$)**	**θ**	**IE%**
Blank	-	13.90	-	-
EEH	200	4.30	0.691	69.1
	600	2.75	0.802	80.2
	1000	2.00	0.856	85.6
	1400	1.10	0.921	92.1
	1800	0.50	0.964	96.4
	2200	0.45	0.968	96.8

The performance of the extract may be the result of the adsorption of the active molecules on the metal surface. These molecules cover the active sites until the surface is saturated, and form a barrier that reduces the reactivity of the metal.

3.2.2. Effect of temperature

Most chemical and electrochemical reactions become faster with temperature rise. It has been shown that few molecules maintain their inhibitory power at elevated temperatures, due to modifications in the form of the inhibitor or in its mode of adsorption at the metallic surface, in a given corrosive environment.

We conducted gravimetric measurements in the corrosive solution without and with the addition of 1800ppm of the EEH extract at various temperatures to evaluate its impact on the extract's performance. Table 3 groups the values of corrosion rate and inhibition efficiency.

Table 3. Corrosion rates of zinc at various temperatures in the absence and presence of 1800 ppm of EEH extract and the corresponding inhibition efficiencies

	Blank	**EEH**	
T(K)	CR (mg/h.cm^2)	CR (mg/h.cm^2)	IE%
298	13.9	0.5	96.4
308	30.8	4	87.01
318	59.05	12.3	79.17
328	91.65	42.4	53.37

We observe that CR of zinc in the uninhibited environment increases with temperature rise, indicating an increase in metallic dissolution. The corrosion rate increases also with temperature after the addition of the extract, but the dissolution is less pronounced compared to the blank, and CR takes lower values.

Regarding the rise in temperature, its leads to a decrease in the inhibition efficiency of the extract. This behavior can be attributed to the fact that the increase in temperature changes the adsorption-desorption balance in favor of the desorption process, and leads to the decrease of the inhibitor performance and the destruction of the protective layer generated on the surface of the metal.

3.3. Electrochemical measurements

3.3.1. Open circuit potential

The evolution of the electrode potential as a function of exposure time to the corrosive solution without and with the addition of 1400 ppm and 1800 ppm of EEH extract at 298 K are represented in Figure 2.

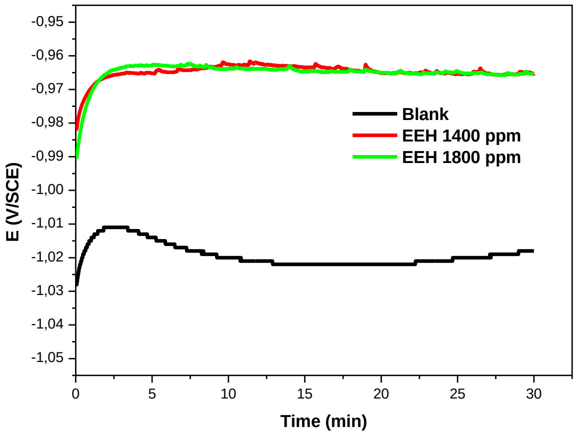

Figure 2. Open circuit potential curves of zinc in uninhibited and inhibited solutions at 298K

By analyzing the curves, we notice that in the inhibited solutions, the potential stabilizes at anodic values compared to the test performed in the uninhibited solution.

This stability reveals the generation of a protective layer resulting from the adsorption of extract molecules on the zinc surface.

3.3.2. Potentiodynamic polarization

Figure 3 illustrates the variation of log (I) as a function of the applied potential to the working electrode in 0.5 M HCl solution at 298 K, without and with the addition of 1400 and 1800ppm of the EEH extract.

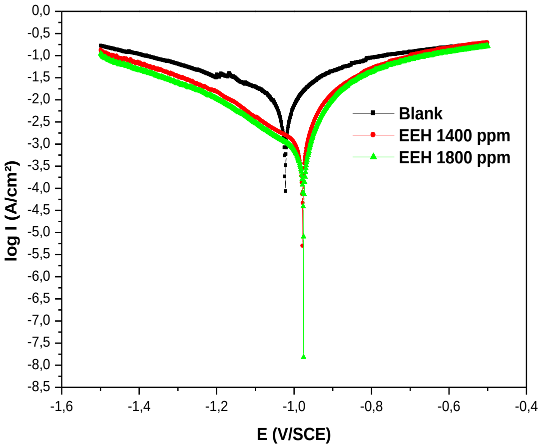

Figure 3. Tafel curves of zinc in 0.5 M HCl solution without and with EEH extract at 298K

The zinc polarization curves show that the cathodic portion is affected by the addition of the extract in the 0.5M HCl solution, indicating that the cathodic reaction is inhibited. We also notice the presence of two successive slopes in this portion of the curve. When the potential exceeds a certain value, the cathodic current density increases rapidly. This growth takes place when the adsorbed molecules desorb from the metallic surface. This potential is called the desorption potential Ed, [21], or non-polarizability potential [22].

However, even though the inhibitor desorbs from the metal surface, it partially inhibits corrosion since the cathodic current densities remain slightly lower than the blank. This clearly indicates that inhibitor adsorption and desorption are dependent on the electrode potential.

The electrochemical parameters determined from the polarization curves, as well as the corrosion inhibition efficiency values IE (%) are grouped in Table 4.

Table 4. Corrosion parameters of zinc in 0.5M HCl solution without and with EEH extract at 298K and the corresponding inhibition efficiencies

C (ppm)	**E$_{corr}$ (mV/ECS)**	**I$_{corr}$ (mA/cm^2)**	**IE (%)**
Blank	-1020	10.298	-
1400	-977	0.968	90.6
1800	-975	0.606	94.1

According to the data in the table, we notice that in the presence of the extract, the corrosion current density decreases, providing inhibition efficiencies of 90.6% and 94.1% for 1400 and 1800 ppm of the extract, respectively. We also note that the corrosion potential shifts slightly to positive values in the presence of the extract. This shift is insignificant, as the difference is around 45 mV.

On the basis of these observations, the studied extract can be considered as a mixed type inhibitor, with cathodic predominance.

We note that there is reasonable agreement between the results of the gravimetric measurements and the polarization tests. The electrochemical method is still more advantageous, as it gives us information about the inhibition mechanism.

3.3.3. Electrochemical impedance spectroscopy

Figure 4 shows the Nyquist diagrams recorded for zinc in 0.5M HCl before and after the addition of EEH extract at 298K.

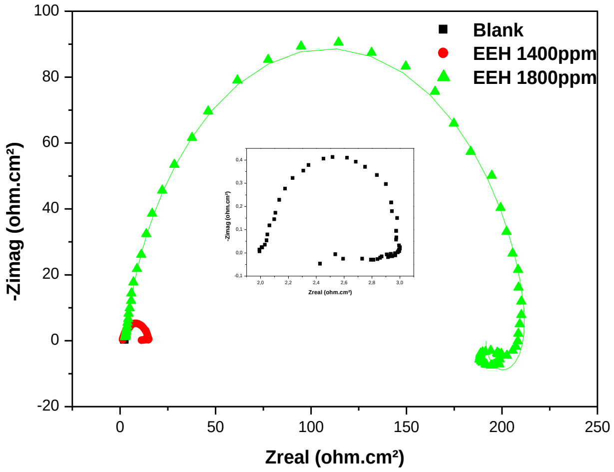

Figure 4. Nyquist diagrams of zinc in 0.5 M HCl solution before and after the addition of EEH extract at 298K

The Nyquist diagrams of zinc in the uninhibited and inhibited solutions show at high frequencies (HF) capacitive semi-circles related to the double layer behavior and the resistance of charge transfer for the corrosion process, followed by inductive loops at low frequencies (LF) resulting from the adsorbed species on the metallic surface, like H^+_{ads} [23] and inhibitor [24], undergo a relaxation process.

The impedance diagrams have a similar shape; however, the diameter of the loop becomes larger with the increase of the extract concentration.

The capacitive loops are slightly depressed as a consequence of the roughness and inhomogeneity of the metallic surface [25].

To fit the impedance diagrams, a suitable equivalent circuit was used. The different parameters were determined and listed in Table 5. Figure 5 shows an equivalent circuit containing the following elements: R_L, R_{ct} and R_s are the inductive resistance, the charge transfer resistance, and the solution resistance, respectively, and L represents the inductance. CPE is the constant phase element.

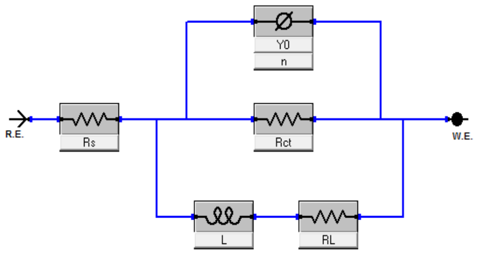

Figure 5. An equivalent circuit model used to fit the impedance diagrams of zinc in the uninhibited and inhibited solutions

The double layer capacitance C_{dl} can be determined from the following formula:

$$C_{dl} = Y_0(2\pi f_{max})^{n-1} \tag{5}$$

where f_{max} is the frequency corresponding to the maximum of the imaginary impedance, Y_0 is the magnitude of CPE, and n is the phase shift.

Table 5. Impedance parameters of zinc in 0.5 M HCl solution without and with EEH extract at 298 K and the corresponding inhibition efficiencies

Conc. **(ppm)**	**R_s** **($\Omega.cm^2$)**	**R_{ct}** **($\Omega.cm^2$)**	**Y_0** **($S^n.\Omega^{-1}.cm^{-2}$)**	**n**	**R_L** **($\Omega.cm^2$)**	**L** **(H.cm²)**	**C_{dl}** **($F.cm^{-2}$)**	**IE** **(%)**
Blank	2.024	0.987	$33.33\ 10^{-5}$	0.891	1.997	8.926	$1.25\ 10^{-4}$	-
1400	1.629	13.429	$16.62\ 10^{-5}$	0.813	81.00	13.41	$4.02\ 10^{-5}$	92.6
1800	2.653	207.501	$0.82\ 10^{-5}$	0.884	1655.64	136.28	$3.59\ 10^{-6}$	99.5

As shown in Table 5, the addition of EEH extract to the corrosive environment enhances the resistance of charge transfer; however, it reduces the double-layer capacitance.

The rise in R_{ct} and the decrease in C_{dl} values are due to the adsorption of the inhibitor on the metal surface and the formation of a protective layer, which reduces the corrosion of the metal [26,27].

A good agreement between the IE values determined from the weight loss, polarization, and impedance measurements was obtained.

3.4. Adsorption isotherm

The inhibition of metals corrosion by organic molecules is the result of the adsorption of these compounds on the metallic surface. It is described by three main types of adsorptions, namely physical adsorption, chemisorption, and mixed adsorption, i.e., physisorption with a tendency to chemisorption or the reverse. Physical adsorption involves the presence of charged species in the solution and a charged metal surface. The chemical adsorption process requires electron transfer or sharing between the unsaturated "d" orbitals of the metal surface and the molecules of the inhibitor allowing the formation of dative bonds and covalent bonds respectively [28].

Inhibitors adsorption on metals can be illustrated through isotherms of adsorption. In order to find the suitable isotherm describing the adsorption of the active molecules of the studied extract, we tested three models (Figure 6), namely: Langmuir, Temkin, and Frumkin. For these isotherms, the coverage rate Θ is related to the concentration of the inhibitor C by the following equations:

Langmuir isotherm $\frac{C}{\theta} = \frac{1}{K} + C$ (6)

Temkin isotherm $\theta = -\frac{lnK}{2\alpha} - \frac{lnC}{2\alpha}$ (7)

Frumkin isotherm $\ln\frac{C\,(1-\theta)}{\theta} = -\ln K - 2\alpha\theta$ (8)

where α is the interaction parameter of adsorbed molecules, and K represents the equilibrium constant of the adsorption process.

The selection of the suitable isotherm, which is presented graphically as a straight line, is dependent on the value of the correlation coefficient.

The variation of Cinh/θ versus the extract concentration is linear, and the value of R^2 for this straight line is closest to unity, implying that the active molecules adsorb on the surface of zinc based on the Langmuir model. As a result, a protective monolayer is formed.

The equilibrium constant is determined from the intercept, and the standard free energy of adsorption $\Delta G°_{ads}$ is calculated using the following formula:

$$K = \frac{1}{10^6}\exp\left(\frac{-\Delta G^0_{ads}}{RT}\right) \quad (9)$$

T represents the absolute temperature, R is the universal gas constant, and 10^6 is the concentration of water in solution (ppm).

In this study, an energy of -21.94 kJ/mol was obtained. The negative value of $\Delta G°_{ads}$ indicates that adsorption of the extract molecules on the zinc surface is a spontaneous process, and leads to the formation of a stable layer. Furthermore, data from the literature [29,30] have shown that values of $\Delta G°_{ads}$ close to or above -20 kJ/mol correspond to physical adsorption of the inhibitor molecules on the metal surface. On the other hand, values close to or lower than -40 kJ/mol correspond to chemisorption.

The value of ΔG° ads is close to -20 kJ/mol. We can deduce that the adsorption mechanism of the extract molecules on the metal surface involves physical interactions.

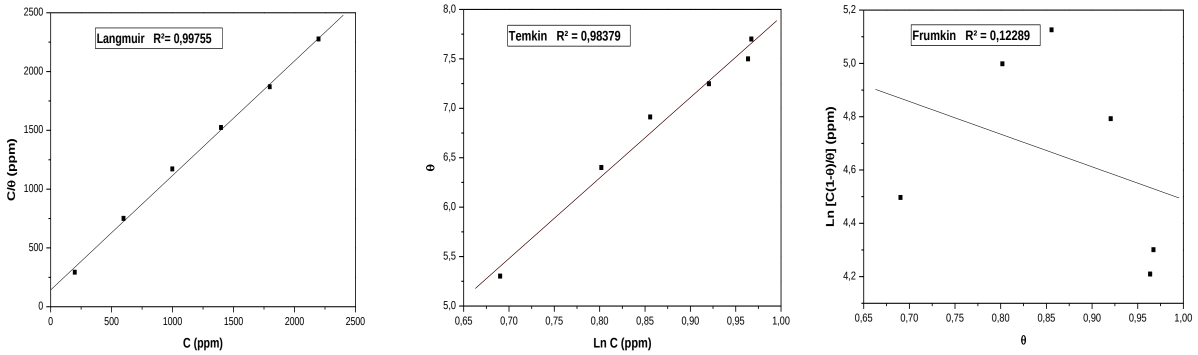

Figure 6. Adsorption isotherms plots for EEH extract on the surface of zinc in 0.5 M HCl at 298K

3.5. Determination of the activation energies

The Arrhenius formula describes relation between the corrosion rate and the temperature:

$$CR = A \exp\left(\frac{-Ea}{RT}\right) \qquad (10)$$

where A represents the Arrhenius constant, E_a represents the activation energy, T is the absolute temperature, and R is the universal gas constant.

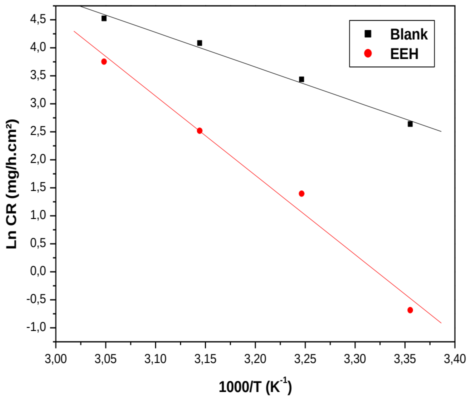

Figure 7. Arrhenius plots for zinc in 0.5M HCl solution without and with 1800ppm of EEH extract

Figure 7 shows the Arrhenius plots for zinc in the uninhibited and inhibited solutions. The activation energies determined from the slopes are shown in Table 6.

Table 6. Activation energy values of zinc in 0.5M HCl solution in the absence and presence of EEH extract

Extract	**Blank**	**EEH**
$\boldsymbol{E_a}$(**kj/mol**)	51.42	117.75

The results in the table show that the activation energy value calculated for zinc in the uninhibited medium is lower than that obtained in the inhibited medium. According to the classification of inhibitors proposed by Radovici [31], and based on the comparison of activation energies obtained without and with the addition of the inhibitor, we can confirm that the active molecules of the EEH extract adsorb on the metallic surface by forming electrostatic bonds. This kind of bonding is sensitive to temperature and does not provide effective corrosion control at high temperatures.

3.6. Synergistic effect

The increase in inhibition efficiency of organic molecules in the presence of specific ions has been observed by several researchers and has been described as a synergistic effect. The adsorption of halide anions on the surface of metals is strong and facilitates the adsorption of organic molecules by forming intermediate bridges between the positive extremity of the organic molecule and the metallic surface, which is also positively charged. The effect of the I^- anion on the performance of EEH extract was examined by gravimetric method. The corrosion rate values determined in the presence of 10^{-2}M KI for different concentrations of the extract and the corresponding inhibition efficiencies are given in Table 7.

Table 7. Corrosion rate, inhibition efficiency, and synergism parameter values for different concentrations of EEH extract in the presence of 10^{-2}M KI

	CR ($\boldsymbol{mg/h.cm^2}$)	**IE**(%)	**S**
Blank	13.9	-	-
KI $\mathbf{10^{-2}}$M	9.45	32.01	-
EEH 600 ppm + KI $\mathbf{10^{-2}}$M	0.9	93.53	2.0785
EEH 1000 ppm + KI $\mathbf{10^{-2}}$M	0.65	95.32	2.0905
EEH 1400 ppm + KI $\mathbf{10^{-2}}$M	0.2	98.56	3.7394
EEH 1800 ppm + KI $\mathbf{10^{-2}}$M	0.05	99.56	6.799

The data presented in the table show an increase in the rate of inhibition with increasing the concentration of the extract in the presence of KI.

The comparison of the inhibition efficiencies obtained without and with the addition of KI is shown in Figure 8.

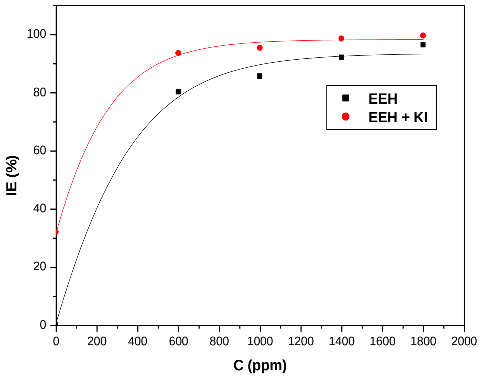

Figure 8. Variation of zinc corrosion inhibition rate as a function of EEH extract concentration in the absence and presence of 10^{-2} M KI in 0.5M HCl at 298K

We can see from the above figure that the inhibition efficiency for different concentrations of the extract takes higher values in the presence of I^- ion, and reaches 99.56% for 1800ppm of the extract. This result shows that the inhibition of zinc corrosion by the mixture is due to a synergistic effect.

The synergism parameter S for various concentrations of EEH extract in 0.5 M HCl is determined from the formula proposed by Aramaki and Hackerman [32,33].

$$S = [(1-\theta_1)(1-\theta_2)]/(1-\theta_{1+2}) \qquad (11)$$

θ_1 is the surface coverage determined in the presence of various concentrations of the extract, θ_2 is the surface coverage determined in the presence of KI, and $\theta_{(1+2)}$ is the surface coverage determined in the presence of various concentrations of the extract with addition of KI. The calculated values of S are given in Table 7.

According to Aramaki [32], the synergistic effect results from cooperative adsorption when a substance is chemisorbed on the metallic surface and another one gets physisorbed on it. But when both the substances adsorb on different sites of the surface, a competitive adsorption occurs. If $S < 1$, the adsorption is competitive, however, in the case where $S > 1$, cooperative adsorption occurs. The values obtained in this study are higher than unity, implying cooperative adsorption between the extract molecules and the I- ion.

4. CONCLUSION

The obtained results revealed that the ethanolic extract of Peganum Harmala seeds (EEH) has very satisfactory anti-corrosive bihavior for zinc in 0.5 M HCl environment. The extract's performance enhances with the increase in concentration and decreases with the elevation of the temperature.The best inhibition rate obtained from gravimetric measurements reached

96.8% in the presence of 2200 ppm of the extract at 298 K. The EEH extract behaves as a mixed-type inhibitor with a cathodic predominance, as demonstrated by potentiodynamic polarization measurements. The inhibition percentages obtained from the electrochemical methods agree with those obtained from the gravimetric method. The corrosion inhibition results from the physical adsorption of the EEH extract molecules on the zinc surface in 0.5M HCl medium following the Langmuir model. The inhibition efficiency of the studied extract was improved in the presence of KI due to a synergistic effect resulting from the cooperative adsorption between the extract molecules and the I- ion.

REFERENCES

[1] A.Y. El-Etre, M. Abdallah, and Z.E. El-Tantawy, Corros Sci. 47 (2005) 385.

[2] R.A. Prabhu, T.V. Venkatesha, B.M. Praveen, K.G. Chandrappa, and S.B. Abd Hamid, Transactions of the Indian Institute of Metals 67 (2014) 675.

[3] M. Boulkroune, Z. Saad Mehenni, S. Beddi, and A. Chibani, Waste Biomass Valor (2023) https://doi.org/10.1007/s12649-023-02145-0.

[4] S.R. Sari, E.N. Sari, Y. Rizky, Sulistijono, and Y. Triana, AIP Conf Proc. 1964 (2018) 020010.

[5] V. I. Vorobyova, M. I. Skiba, A. S. Shakun, and S. V. Nahirniak, Int. J. Corrosion and Scale Inhibition 8 (2019) 150.

[6] M. A. Al-Yahya, Fitoterapia (1986).

[7] S. Tahrouch, S. Rapior, L. Mondolot, L. A. Idrissi-Hassani, J. M. Bessière, and C. Andary, Rev. Biology Biotechnol. 2 (2002) 33.

[8] A. Djemoui, L. Souli, D. Djemoui, M. Okazi, A. Naouri, and S. E. Rahmani, J. Chem. Pharm. Res. 9 (2017) 311.

[9] G. Bahlakeh, B. Ramezanzadeh, A. Dehghani, and M. Ramezanzadeh, J. Mol. Liq. 283 (2019) 174.

[10] I. Ghazi, S. Jorio, S. Mostapha, R. Fdil, and H. El attari, Mor. J. Chem. 9 (2021) 542.

[11] K.A. Al-Saadie, H.A. Abas, H.A.Y. Almashhdani, K.A. Al-Saadie, H. A. Abas, and H.A.Y. Almashhdani, Mater. Sci. Applications 6 (2015) 1061.

[12] H. Abdulameer Abbas, Iraqi J. Sci. 56 (2015) 1836.

[13] N. Al Otaibi, and H.H. Hammud, Molecules 26 (2021) 7024.

[14] H.H. Hammud, S.A. Maache, N. Al Otaibi, and N.S. Sheikh, Molecules 27 (2022) 7250.

[15] J.F. Arteaga, M. Ruiz-Montoya, A. Palma, G. Alonso-Garrido, S. Pintado, and J.M. Rodríguez-Mellad, Molecules 17 (2012) 5126.

[16] P.A. Kilmartin, H. Zou, and A.L. Waterhouse, J. Agric. Food Chem. 49 (2001) 1957.

[17] S. Amidi, F. Mojab, A.B. Moghaddam, K. Tabib, and F. Kobarfard, Iran J. Pharm. Res. 11 (2012) 117.

[18] T. Huang, P. Gao, and M. Hageman, Curr. Drug Discov. Technol. 1 (2004) 173.

[19] A. Borah, S. Selvaraj, S. R. Holla, and S. De, Arabian J. Chem. 15 (2022) 104370.

[20] M.A. Haque, K. Morozova, N. Lawrence, G. Ferrentino, and M. Scampicchio, Electroanalysis 33 (2021) 23.

[21] M. Bartos, and N. Hackerman, J. Electrochem. Soc. 139 (1992) 3428.

[22] H. C. Kuo, and K. Nobe, J. Electrochem. Soc. 125 (1978) 853.

[23] H. J. W. Lenderink, M. V. D. Linden, and J.H.W. de Wit, Electrochim Acta 38 (1993) 1989.

[24] A. K. Singh, and M. A. Quraishi, Corr. Sci. 52 (2010) 152.

[25] W. Schelder, J. Phys. Chem. 79 (1975) 127.

[26] C. Cao, Corr. Sci. 38 (1996) 2073.

[27] W.H. Li, Q. He, S.T. Zhang, C.L. Pei, and B.R. Hou, J. Appl. Electrochem. 38 (2008) 289.

[28] O. Radovico, Proceedings of the 7th European Symposium on Corrosion inhibitors – 153rd Manifestation of the European Federation of Corrosion, University of Ferrara, Italy, 1 & 2 (1991) 330.

[29] M. Boulkroune, and A. Chibani, Chem. Sci. Trans. 1 (2012) 355.

[30] M. Sahraoui, M. Boulkroune, A. Chibani, Y. Larbah, and A. Abdessemed, J. Bio. Tribocorros. 8 (2022) 1.

[31] A. Popova, E. Sokolova, S. Raicheva, and M. Christov, Corr. Sci. 45 (2003) 33.

[32] K. Aramaki, M. Hagiwara, and H. Nishihara, Corr. Sci. 27 (1987) 487.

[33] K. Aramaki, and N. Hackerman, J. Electrochem. Soc. 116 (1969) 568.